Original Research Article

Development and preliminary analysis of a solar dryer for flour dehydration

ABSTRACT

Until now, drying flour in full sunlight has been the technique most widely used in Burkina Faso. This method exposes the flour to numerous risks of poisoning, pollution, soiling and destruction of nutritional qualities. Despite this, there are very few documented solutions to the problem. This has prompted this work on the design and preliminary study of a solar dryer for drying flour. To this end, the design approach based on unfavourable periods was used to dimension the solar collector elements. The initial studies were carried out experimentally, starting with a no-load study and then a load study. As a result of this work, a two-in-one solar dryer was designed and built. It was able to heat the drying air to 65°C in unfavourable weather conditions. During drying, the temperature reached 58°C in forced convection. However, the average drying temperature was below the predefined drying temperature range (45-55°C). The drying speed was less than half that predicted. As a result, the drying time was 10 hours 20 minutes instead of the planned 4 hours. The water content lost by the flour reached 31.14% on rack 1

Keywords: solar dryer, flour, preliminary, design, drying rate and moisture content

1. INTRODUCTION

Drying is one of the oldest operations instinctively applied whenever humans need to preserve a body that is initially moist for a long time. It is the oldest method of food preservation, as noted by (Ojediran & Raji, 2010), (N. Ahmed et al., 2013), (Harrison & Andress, 2000), (Jayas, 2016). At a distant stage of technologicaldevelopment, sun drying, referred to as traditional drying, and smoking were the mostcommonlyusedmethods to obtain dry products(Burgos, 2003). Although sun drying is less expensive**,** it is not well-suited to agri-food products. Several studies have easily demonstrated this (Mishra et al., 2020). Smoking, which adapts only to a limited number of food products, is also very energy-intensive, as it requires temperatures above 85 °C (Nizio et al., 2023) and takes a long time. The advent of dryers has redistributed the roles in the drying of agricultural products. A significant number of drying technologies have been developed, as evidenced by their abundance in the scientific literature. This is justified by the complexity of drying and the specific needs for energy, temperature, air renewal, relative humidity, and drying duration.

In Burkina Faso, especially in rural areas, the staple food is to. A dish made from corn or millet flour (sorghum and small millet). However, for the vast majority of households, flour is still dried in the open air under the sun. This exposes it to dust, animals, insects, and potential contamination. Moreover, drying in the open air and under the sun may alter the

nutritional quality of the products (A. Ahmed et al., 2023) and (Mohammed et al., 2020) including flour, as the thermal conditions are uncontrolled and uncontrollable. Furthermore, (Alam et al., 2019) found that the loss due to sun drying paddy averages 3.1%, compared to only 0.39% for machine drying. Similarly, (Roy et al., 2020) reveal that the average loss from sun drying is 2.12% ± 1.24% compared to the drying in the solar dryer S4S, which is only 0.41% ± 0.55%. Aware of these situations, some households attempt to dry their products indoors to avoid dust and protect against predators (poultry and animals). In this case, improper drying often occurs due to insufficient ventilation and/or excessive relative humidity of the drying air. Therefore, it is necessary to find an effective and accessible means for flour drying, as this concerns the health of the population. This has motivated the development and experimental analysis of a solar dryer specifically for flour.

To this end, a disadvantaged period approach has been adopted for the design calculations. That is to say, the period with low values of the central parameter, such as the thermal solar flux in the present study. After construction, the dryer was first tested empty to evaluate its capacity to heat the air, and then under load to study the drying process.

2. MATERIALS AND METHODS

The equipment used is a "midi LOGGER GL220" datalogger, thermocouples (as used by (Boukaré et al., 2024)), a UNI-T UT330B IP67 hygrometer Fig.1 (a) and an SF-550 electronic balanceFig.***1*** (b).

Fig.1. (a) hygrometer and (b) electronic *scales*

2.1. Design methodology and construction

2.1.1. Calculation assumptions and hypotheses

The aim is to build a mobile solar dryer that takes up less space and is able to operate both during periods of favourable solar thermal flux and during periods of unfavourable solar thermal flux. With the exception of August, when there is too much cloud cover, the period of low solar thermal flux lasts from the end of November to mid-February of the following year. We therefore adopt the idea of 'two in one' by combining the solar collector and the drying chamber. The disadvantaged period approach is also used for the solar thermal flux. The food to be dried is grain flour (millet, sorghum, maize, wheat, rice, etc.).
The drying temperature will be between 45 and 55°C because the water contained in the flour is that of wetting, i.e. unbound water. It will not be insulated for the simple reason that the 45-55°C drying temperature range is not very far from the ambient temperature, which often reaches 45°C in the shade. The other assumptions and considerations are set out in Table 1.

Table 1. Design data

Parameters	Conditions
Location and latitude	12,2

Product	Corn flour
Capacity	10 kg
Density	0,49-0,56 g/ml
Maximum drying temperature	45-55°C
Initial moisture content	25 %*
Final moisture content	13 %
Thickness of flour layer	4 cm
Drying time	4 hours
Period	Except August
Ambient temperature	32°C
Incident solar irradiation	600W/m2
Type of collector	Flat plate solar thermal collector
Tilt angle of solar collector	42,2°
Author of the dynamic vienne	5 cm
Type of absorber	Aliminium painted black
Absorber thickness	0,30 mm
Type of glass	Clair
Thickness of glass	5 mm
Type of insulation	No isolant
Number of racks	2 racks
Distance between racks	20 cm

2.1.2. The mass of water to be evaporated

It is the preferred generic model used by a large number of researchers (Khalifa et al., 2012), (Babar et al., 2020), (Abubakar et al., 2018),(Khan et al., 2011),(Musembi et al., 2016)

$$M_w = W_p \times \frac{(M_i - M_f)}{(1 - M_f)} \quad (1)$$

W_p : product mass
M_w :mass of water to be evaporated
M_i:initial moisture content
M_f:final moisture content

$$M_w = 25 \times \frac{(0{,}25 - 0{,}13)}{(1 - 0{,}13)} \Longrightarrow M_w = 3{,}45kg$$

2.1.3. Volume of drying air

The volume of drying air is calculated according to the model used by (Forson et al., 2007)

$$V_{air} = \frac{M_w \times L_t \times R_a \times T_a}{C_{P_{air}} \times P_{at} \times (T_c - T_f)} \quad avec\ T_f = T_a + 0{,}25\Delta T \quad (2)$$

with
$C_{P_{air}}$ the specific heat of the air (J/(kg K)).
R_a the perfect gas constant (J/(kg K)). Air is assumed here to be a perfect gas.
L_l is the latent heat of vaporisation.
T_a the ambient temperature
T_f air temperature at the outlet of the drying bed (°C)
T_C drying temperature (°C), P_{at} atmospheric pressure, (N/m^2)

$$Cp_{air} = 1{,}005kj/kg$$

$$L_l = 2257kj/kg$$

$$V_{air} = \frac{M_w L_l R_a T_a}{Cp_{air} \times P_a \times (T_C - T_f)}$$

$$V_{air} = \frac{3{,}45 \times 2257 \times 0{,}287 \times 32}{1{,}0005 \times 101325 \times (55 - 36{,}39)}$$

$$V_{air} = \frac{71512{,}5936}{1895086{,}54125}$$

$$V_{air} = 0{,}0377357 m^3 \cong 0{,}038 m^3$$

2.1.4. Expression of air mass m_{air}

Knowing the volume of air V_{air}, we can deduce its mass by:

$$m_{air} = V_{air} \times \rho_{air} \qquad (3)$$

$\rho_{air}$is the density of air. We use the one presented by (Forson et al., 2007) to find the air mass using the equation …

$$m_{air} = \rho_{air} \times \frac{M_w \times L_t \times R_a \times T_a}{C_{P_{air}} \times P_{at} \times (T_c - T_f)} \qquad (4)$$

2.1.5. Useful power transmitted by the solar collector to the heat transfer fluid

It is a function of the power of the solar radiation incident on the sensor and its optical properties.

$$P_u = S \times \varepsilon P_a \; avec \;\; P_a = \alpha P_v \;\; et P_v = \tau P_i \;\; \Longrightarrow \;\; P_a = \alpha\tau P_i \;\; \Longrightarrow P_u = S \times \varepsilon\alpha\tau P_i$$

P_u useful power (W)

P_a the power collected by the solar collector absorber (W/m^2)

P_v the power transmitted by the glass (W/m^2), P_i the power or incident solar radiation (W/m^2)

$S$the heat exchange surface or the surface of the solar collector (m^2)

α the absorbtivityε the emissivity and τ the transmittivity. The last three are adimensional numbers.

2.1.6.Incidence angle or tilt angle of the solar collector

The tilt angle (β) of the solar collector has been discussed by several authors, as pointed out by (Stanciu & Stanciu, 2014). Expressions of tilt angle as a function of latitude φ regularly encountered include: 10° + φ(Yusuf Abdullahi, 2013), $\varphi \mp 15°$(Duffie et al., 1985), φ – 10°(Heywood, 1971), 0,917φ + 0,321(Moghadam et al., 2011), φ + (10 … 30°)(Löf & Tybout, 1973)

To takeaccount of the idea of "two in one", i.e. solar collector and drying chamber in one unit, and to optimise the drying surface area, we are forced to have a relatively high inclination. In thiscontext, the model of (Löf & Tybout, 1973) will be chosen..

$$\beta = \varphi + 30° = 12.2 + 30° = 42.2°$$

2.1.7.Heat of the drying air

The energy used to dry the flour is the energy received by raising the temperature of the drying air. It is therefore called useful energy and is expressed by the equation …

$$E_u = m_{air} \times C_{P_{air}}(T_c - T_a) \qquad (5)$$

With m_{air} $en\ kg$; $C_{P_{air}}$ $en\ J/kg$ ℃ ; T_c = 55℃ et T_a = 32℃

T_c is the collector or absorber temperature and T_a is the ambient temperature.

2.1.8. Solar radiation collection surface

By identifying the basic relationship of the unit of measurement of energy in the International System of Units (SI) (E= Pxt) with the useful energy received from the sun by the drying air, we deduce the surface area of capture (S) Eq (6)

$$P_u \times t = E_u \Leftrightarrow E_u = \varepsilon\alpha\tau P_i \times S \times t$$

$$\Longrightarrow \quad S = \frac{E_u}{\varepsilon\alpha\tau P_i \times t} = \frac{m_{air} \times C_{P_{air}}(T_c - T_a)}{\varepsilon\alpha\tau P_i \times t} \qquad (6)$$

By replacing the mass of drying air m_{air}in (6) :

$$S = \rho_{air} \times \frac{M_w \times L_t \times R_a \times T_a \times (T_c - T_a)}{\varepsilon\alpha\tau P_i \times P_a \times (T_c - T_f) \times t} \qquad (7)$$

Like $T_f = T_a$ + 0,25ΔT avec $\Delta T = 2\beta(T_b - T_S)\frac{P_i}{P_0}$

T_b =Boiling temperature and T_S= solidification temperature.

P_0 = 1367$W/m^2\beta\epsilon$0,14 – 0,25(Forson et al., 2007)

So S becomes:

$$S = \frac{\rho_{air} M_w L_t R_a (T_c - T_a)}{t \times \varepsilon\tau\alpha P_i \, (T_c - (T_a + 0{,}25 \times \Delta T))}$$

T_a = the ambient temperature of the drying room.

$$\Delta T = 2\beta(T_b - T_S)\frac{P_i}{P_0}$$

$$S = \frac{\rho_{air} M_{co} L_f R_a (T_c - T_a)}{t_\alpha \varepsilon\alpha\tau P_i \left[T_c - T_a - 0{,}25 \times 2 \times 0{,}25(T_P - T_s)\frac{P_i}{P_0}\right]}$$

P_i = overall power incident on a horizontal surface.

ρ_{air} = 1,29/m^3(Babar et al., 2020)

Numerical application

$$\Delta T = 2 \times 0{,}20 \times 100 \times \frac{600}{1361} = 17{,}5$$

$$\Delta T = 17{,}56°C$$

$$\tau = 0{,}78$$

$$T_f = T_a + 0{,}25\Delta T = 32 + 0{,}25 \times 17{,}56 = 36{,}39°C$$

$\varepsilon \in [0{,}86 - 91]$ We take 0.86, the most unfavourable

$$\alpha = 0{,}97$$

$$L_l = 2257kj/kg$$

$$S = \frac{1{,}29 \times 3{,}45 \times 225710^3 \times 0{,}287 \times (55 - 32)}{4 \times 3600 \times 0{,}78 \times 0{,}86 \times 0{,}97 \times 600(55 - 36{,}39)}$$

$$S = \frac{66.305.582{,}8785}{104622434{,}3104}$$

$$S = 0{,}63376 \cong 0{,}64m^2$$

2.1.9. Determining the dimensions of the flat plate collector

The flat-plate solar collector is rectangular in shape. Then we have:

$S = L \times l$ (8)

According to (FORSON, 1999) quoted by (Forson et al., 2007) the ratio between the length of the solar collector and its width of 1.5 is recommended for optimal performance.
This means that

$$\frac{L}{l} = 1{,}5$$

$$L = 1{,}5 \times \frac{s}{L}$$

$L = 1{,}5 \times \frac{S}{L} \Longrightarrow L = \sqrt{1{,}5 \times S}$ (9)

$$L = \sqrt{1{,}5 \times 0.64} = 0.98\,m$$

$$L = 1m$$

$$l = \frac{0{,}64}{0{,}98} = 0{,}65306122 \backsimeq 0{,}65m$$

$$l = 0{,}65\text{m}$$

2.1.10. Air change rate

The drying air flow rate is the ratio of its volume to the expected drying time.

$Q_V = \frac{V_{air}}{t}$ (10)

The desired drying time is 4 hours. $V_{air} = 0{,}038\,m^3$

$$Q_v = \frac{0{,}038m^3}{4h} = 0.0095m^3.h^{-1}$$

2.1.11. Ventilation power

It is calculated using the formula:

$P_v = \frac{1}{\eta_v}\frac{Q_V}{3600}\Delta P_t$ (11)

With:

Q_V: required flow in m^3/h;

η_v : Fan efficiency in accordance with supplier's specifications;

3600 : hour/second conversions;

ΔP_t total pressure drop in Pascals.

2.2. Drying maizeflourproceding

2.2.1. Preparing the flour

The quality of the flour depends directly on the quality of the cereals used. So, to guarantee the best quality, a protocol for processing the cereal until the flour is obtained has been clearly defined. The cereal must undergo the followingoperations:

- winnowing and sorting: the quantity of cereal to be processed must be winnowed and sorted to remove all kinds of impurities (foreign bodies and mouldy grains);
- moistening: after winnowing and sorting, the grains are slightly moistened by suction to allow hulling;
- winnowing and sifting: this stage first removes the bran from the hulled grains, and then separates the grits from the coarse fraction of the flour;
- soaking (Fig.2(a)): the resulting product is then soaked in water for around 24 hours to make it easier to grind;
- draining/washing (Fig.2(b)): the wet product is drained using a plastic sieve or clean basket, then washed again with clean water;
- Grinding: the wet product is ground to obtain flour.

Fig.2. (a) Soaking (b) Draining

2.2.2.Moisture content and moisture ratio

The flour was spread out on a mat on each of the two racks, as shown at **Fig.3**
The flour on each rack was weighed at one-hour intervals, as shown in the diagram. The moisture content on a wet basis at each point in time was calculated using the following formula: as employed by(Adelaja & Babatope, 2013)

$X_t = \frac{m_i - m_t}{m_i} \times 100$ (12)

Avec :$m_t$the mass of flour at each moment,$m_i$the mass of wet flour and$X_t$the moisture content of the flour at each moment.
The moisture ratio is assessed using the model used by(Sehrawat & Nema, 2018)

$MR = \frac{m_t}{M_i}$ (13)

2.2.3. Drying rate

The flour drying rate is evaluated by the Eq. (14) used in numerous works such as (Adelaja & Babatope, 2013)
Average drying speed

$DR = \frac{m_e}{t_s}$ (14)

DR : drying rate ($en\,kg/h$);
t_s : drying time for the product in question (in hour).
m_e : mass of water to be extracted from the product ($enkg$).

The different flour masses are obtained by weighing as shown in**Fig.4**

Fig.3. Flour drying

3. RESULTS AND DISCUSSIONS

3.1. Prototype solar dryer

Fig.4. Weighing the flour

The solar dryer designed (**Fig.5**) and built (**Fig.6**) consists of a flat solar collector, a drying chamber, a 24 cm chimney, supports and wheels. The solar collector consists of a surface that is transparent to the sun's rays: the pane, and an opaque surface: the absorber. In between is the dynamic pane. The absorber is pierced by two rows of holes (**Fig.6**) corresponding to the entrance to each rack, to allow the drying air to pass over the layer of flour. The drying chamber is equipped with two shelves. They are 30 cm apart. The upper rack is 55 cm long and 50 cm wide and the lower rack is 87 cm long and 50 cm wide.

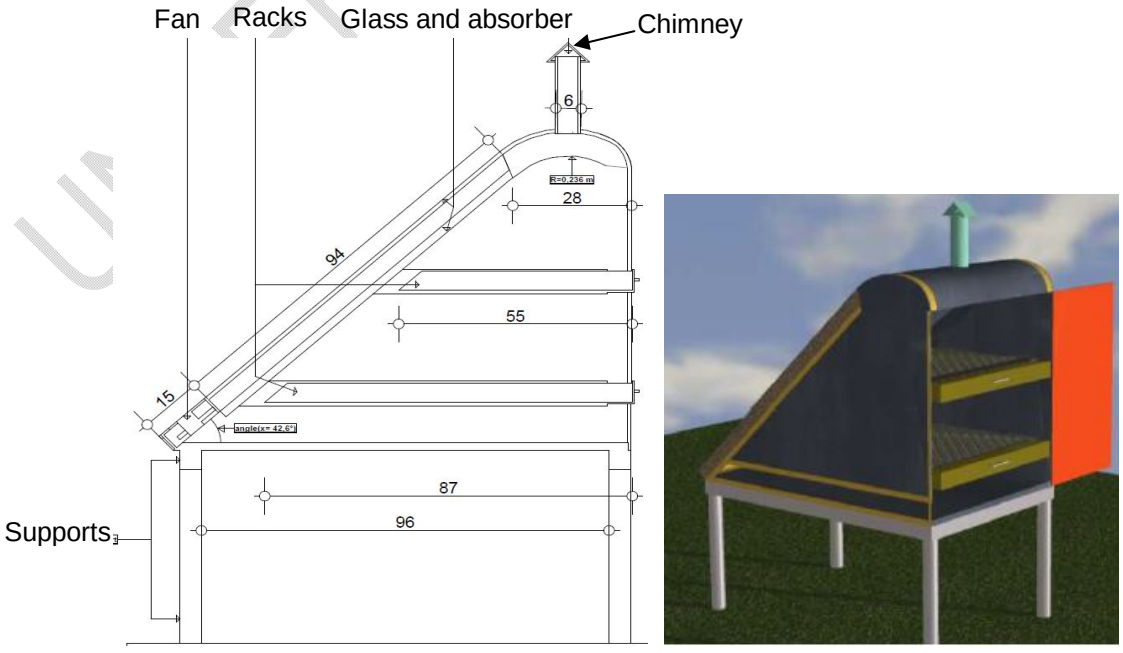

Fig.5. Model of dryerdesigned

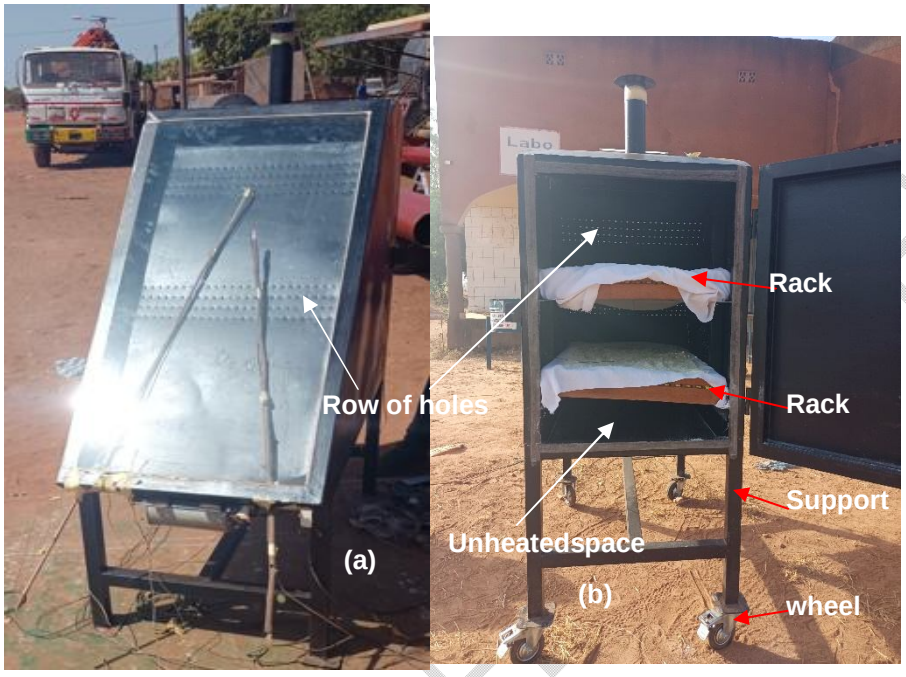

Fig.6Dryerbuilt in instrumentation

3.2. Temperature and relative humidity

3.2.1. No-load test

Before the drying operation, the dryer was tested empty and under natural convection to verify the temperature increase in the drying chamber. Three tests were conducted, and the results are presented in **Fig.7**, 8, and 9. These tests took place on 25th and 29th November, as well as on 1st December 2023. It is observed that the temperature at the level of rack 1 is higher than that at the level of rack 2. This is due to the fact that the inlet of rack 2 is closer to the air inlet of the solar collector (**Fig.6**). For test 1 (**Fig.7**), the maximum temperature reached is 65.1 °C at 13:29. The minimum temperature recorded is 43.8 °C at 16:15, and the average temperature is 58.56 °C. On rack 2, the maximum, minimum, and average temperatures are 57.6 °C at 12:39, 40.8 °C, and 52.25 °C, respectively. During the second test (**Fig.8**), rack 1 recorded a maximum temperature of 55.1 °C, a minimum temperature of 35.7 °C, and an average temperature of 48.67 °C. rack 2 recorded a maximum temperature of 51 °C, a minimum temperature of 32.7 °C, and an average temperature of 44.57 °C. For test 3 (**Fig.9**), the recorded temperatures are 58.8 °C max, 35.1 °C min, and 51.01 °C on average for rack 1, and 55.2 °C max, 34 °C min, and an average of 48.46 °C for rack 2. The temperatures appear to fall within the range of 45 to 55 °C recommended for flour drying. However, under forced convection, they might drop below this threshold, as they spend less time in the dynamic phase. It is also noted that the temperatures in the racks are significantly different from the ambient temperature, indicating that the heat transfer fluid is primarily heating up. (Lingayat et al., 2017) found similar temperature profiles and solar radiation, with

peaks larger than ours. Similarly, (Krabch et al., 2022) observed the same pattern, but with maxima close to those in this study as they required low temperatures, as is the case in this work.

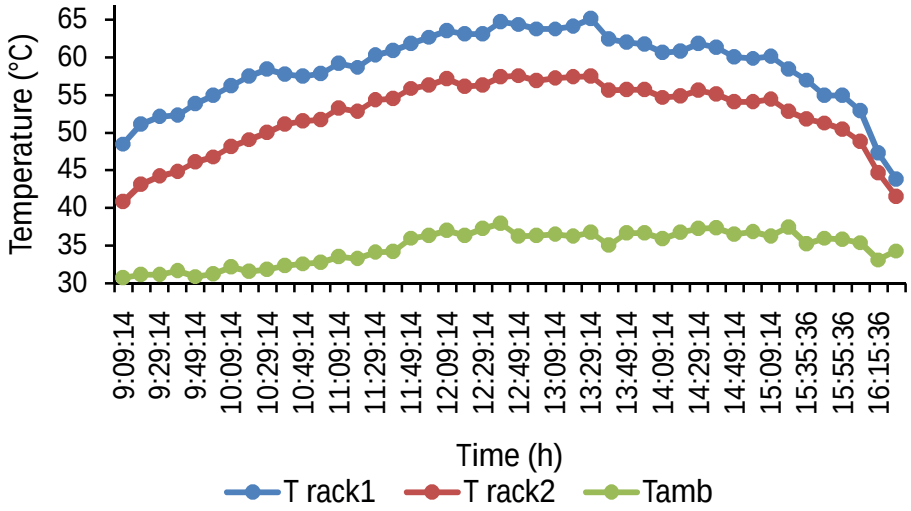

Fig.7. Temperature changes in the drying chamber during the test1

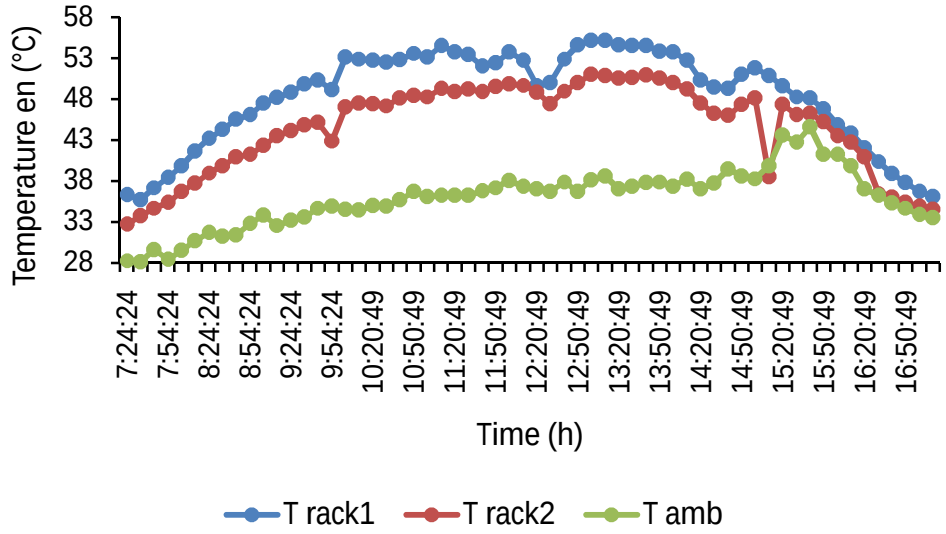

Fig.8. Temperature variations in the drying chamber, test2

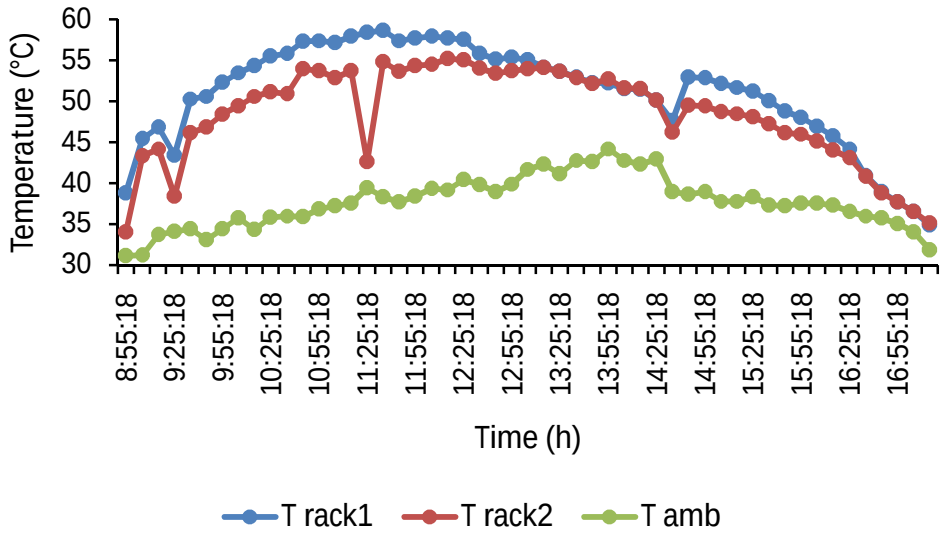

Fig.9. Temperature trends in the drying chamber, test3

3.2.2. Laod test

The temperatures of the drying air in the racks during the drying operation are shown in **Fig.10** and 11 for the two tests respectively. Test 1 was carried out over two days: 27 and 28 November 2023. On the first day, it can be seen that the air was unable to heat up properly, as the average temperature was below 40°C. As a result, the test started late.

On the second day, the drying air in rack 1 heated up well, while that in rack 2 remained superimposed on the ambient temperature for most of the time (see **Fig.10**). This indicates that it did not heat up sufficiently. This could explain the long drying time (around 16 hours of discontinuous drying).

In test 2 (see **Fig.11**), the temperature in rack 1 increased more effectively than in rack 2, with an average of 46.42°C and a peak of 53.2°C. However, it remains limited, as the required drying temperature range is between 45 and 55°C. It can still be seen that rack 2 has a temperature that is almost the same as, and at times even lower than, the ambient temperature. This could justify reducing the ventilation speed, as rack 2, located further away from the sensor air intake, has an average temperature close to the lower limit of the drying temperature range. In addition, there is a volume of air below this rack (see **Fig.6**), which could contribute to its cooling.

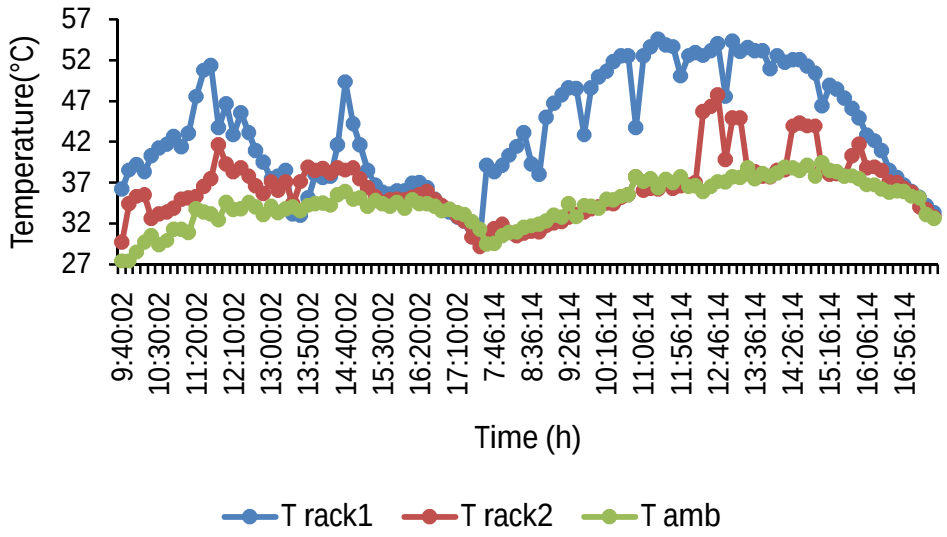

Fig.10. Drying air temperatures in drying test1

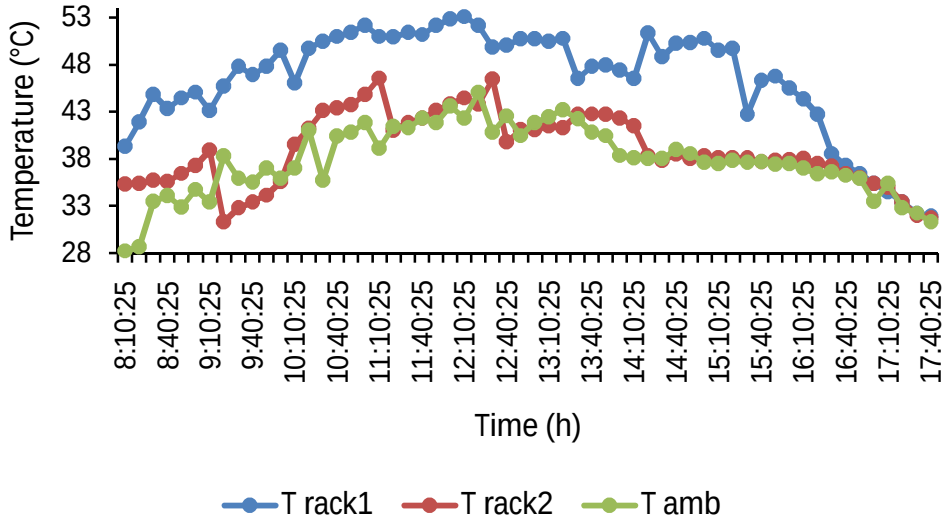

Fig.11 Variation in drying air temperature at the Drying Test2

Drying depends not only on thermal conditions, but also on humidity and pressure parameters, which are measured to analyse hygrometric and barometric conditions. The results are shown in **Fig.12** and 13. Test 1 (**Fig.12**) shows that on the first day of drying, the relative humidity, which was 79.5 %, fell to 49.4 % around 4 p.m. and rose again to 84.9 % at 7 p.m. during the night. This shows that the flour had become moist. This could be due to the thermal inertia of the flour, which has stored the heat received, giving it a higher temperature than the air between 5 pm and 7 pm. This allows moisture to be transferred from the fresh air to the flour. It drops later in the night, perhaps as a result of uninterrupted forced convection. In the second test (**Fig.13**), relative humidity and pressure decreased with drying time, indicating that water evaporation was decreasing. It should also be noted that **Fig.12** and 13 show that relative humidity falls at the time of maximum temperature, as found by (Krabch et al., 2022).

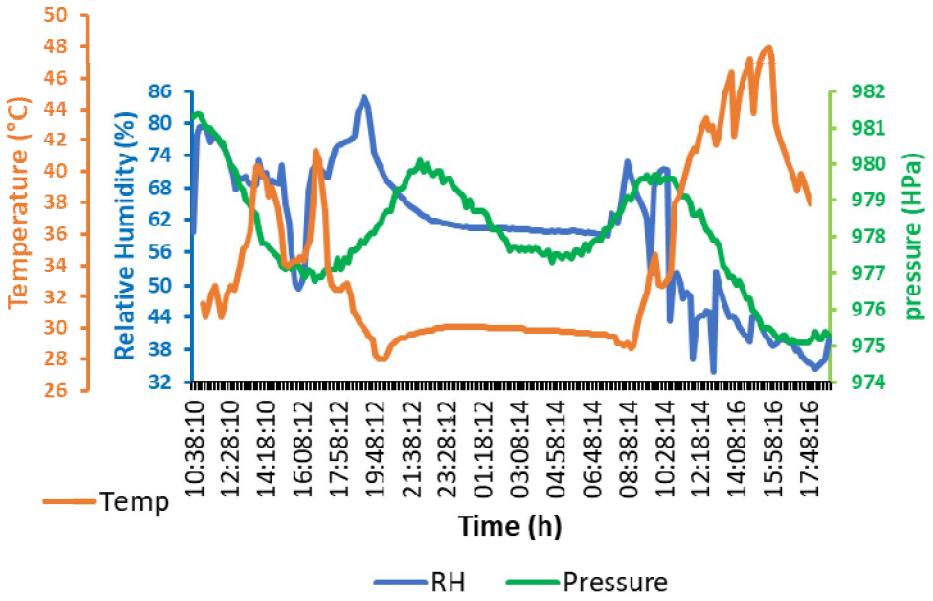

Fig.12. Pressure, Humidty of air drying in Test1 of drying

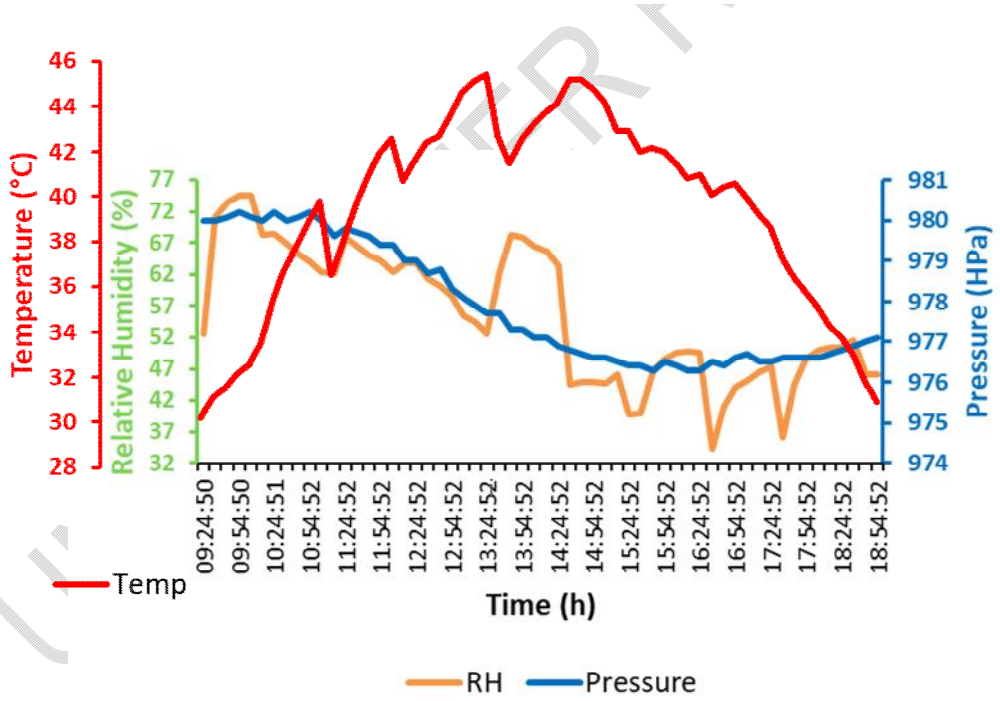

Fig.13. Pressure, relative humidity of the drying air at the drying Test2

3.3. Moistureloss and moisture ratio

The mass of water lost or the moisture lost by the flour during drying is presented in **Fig.14** and 15. It is observed that the amount of water released increases with drying time and stabilises to mark the end of the operation. This is somewhat the opposite of what was found

by (Khan et al., 2011), who observed a linearly increasing trend. The flour in rack 1 releases more water than that in rack 2, despite its lower quantity. This could be explained by the amount of energy received at the two racks. Indeed, rack 1 receives more heat than rack 2, as the air entering rack 2 is cooler than that in rack 1, which is closer to the air inlet in the solar collector. **Fig.14** shows two phases, separated by a transitional phase. The first phase corresponds to the first two days of drying, while the second is related to the effect of forced ventilation during the night. Differentiation indicates that 7.43% and 8.09% of water were released at night from rack 1 and rack 2, respectively. These significant amounts of water are released solely due to the effect of forced convection. The maximum amount of water lost from rack 1 is 31.14% and 25.22% from rack 2 (**Fig.14**). During the second test (**Fig.15**), the maximum water content lost from rack 1 and rack 2 is 23.21% and 21.14%, respectively. Furthermore, **Fig.16** and 17 show the evolution of the ratio of the water content of the flour during drying. It is noted that this ratio decreases over the drying time and is dependent on the rack, thus on the amount of heat and the humidity of the drying air, as it does not have uniform thermal or hygrometric characteristics between the racks.

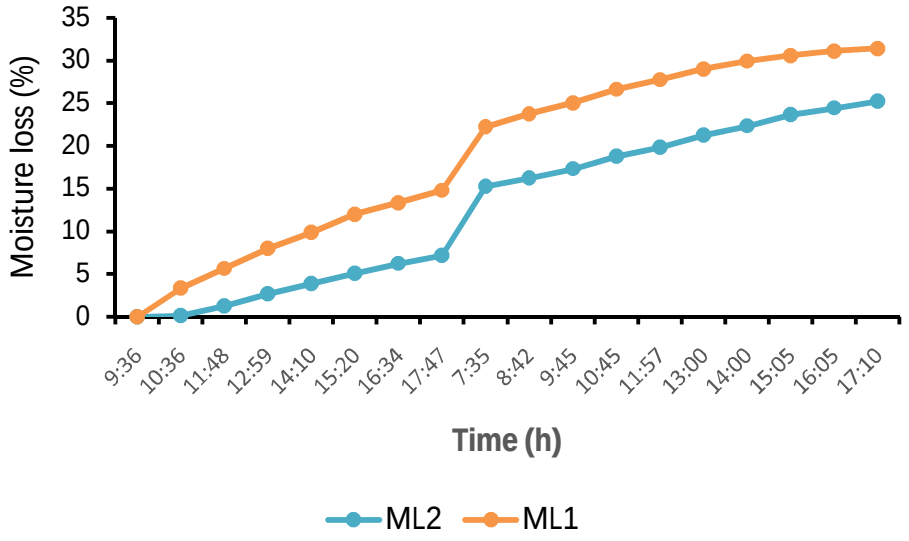

Fig.14. Evolution of the moisture content lost by flour during drying, Test1

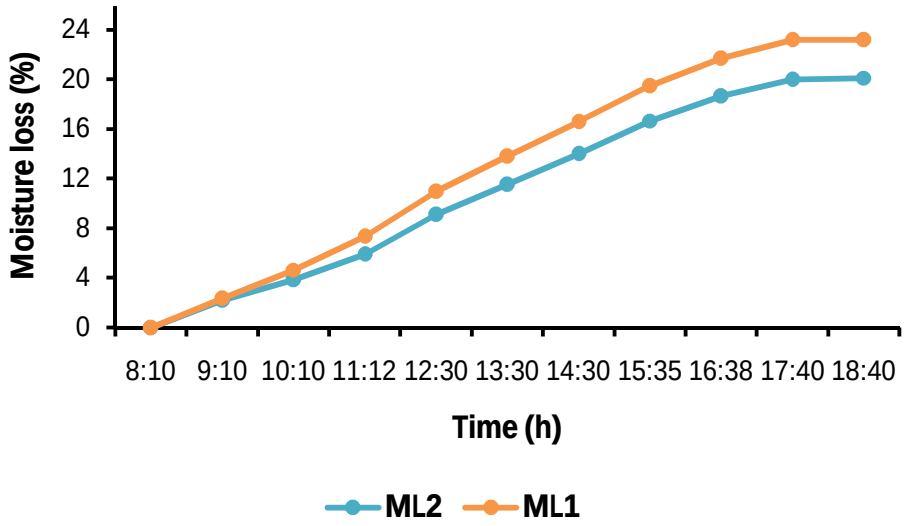

Fig.15.Variation in moisture content lost from flour during drying, Test2

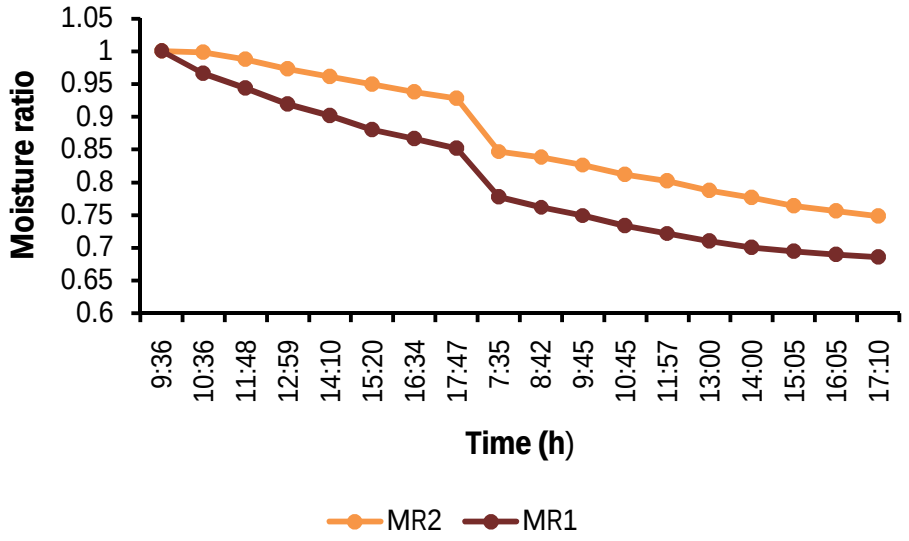

Fig.16.Moisture ratio evolution during drying time, Test1

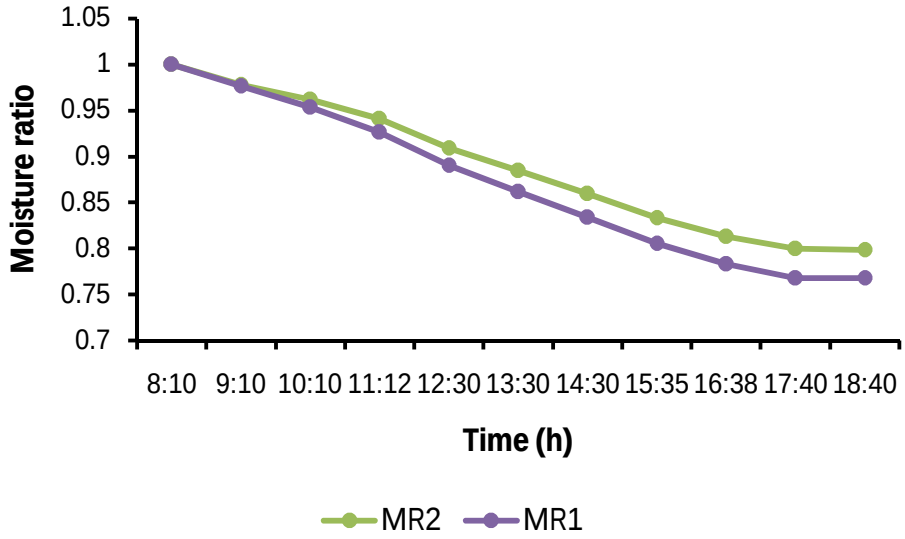

Fig.17. Moisture ratio variation during drying time, Test2

3.4. Drying rate

The drying rate or speed is shown in **Fig.18** and 19 for tests 1 and 2 respectively. **Fig.18** shows that there are two phases, each corresponding to two days of drying. The drying rate decreases dramatically with drying time on rack 1. For rack 2 the trend is less clear on the second day of drying. The drying rate for Test 2, shown in **Fig.19**, shows a completely different trend to that of Test 1. It decreases and then continues to decrease, reflecting a bell-shaped trend with a peak of 0.101 kg of water per kg of dry matter per hour at about 12 h 30 min and 0.093 101 kg of water per kg of dry matter per hour for Rack 1 and Rack 2 respectively. When the rate cancels out or tends to zero, this indicates the end of drying.

Fig.19 shows that the drying time was 10h20 min, more than double the expected time (4 hours). This could be due to the low heating of the drying air.

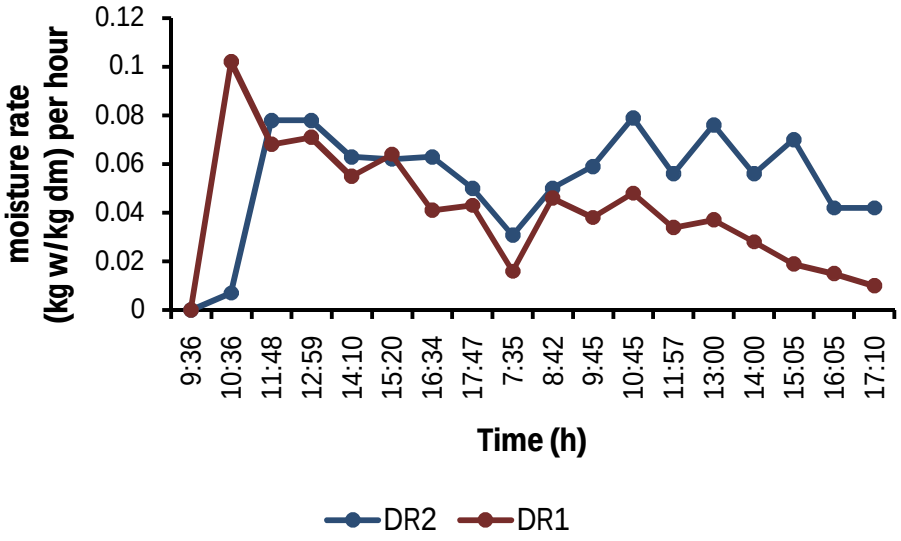

Fig.18. Drying rate evolution with the time Test1

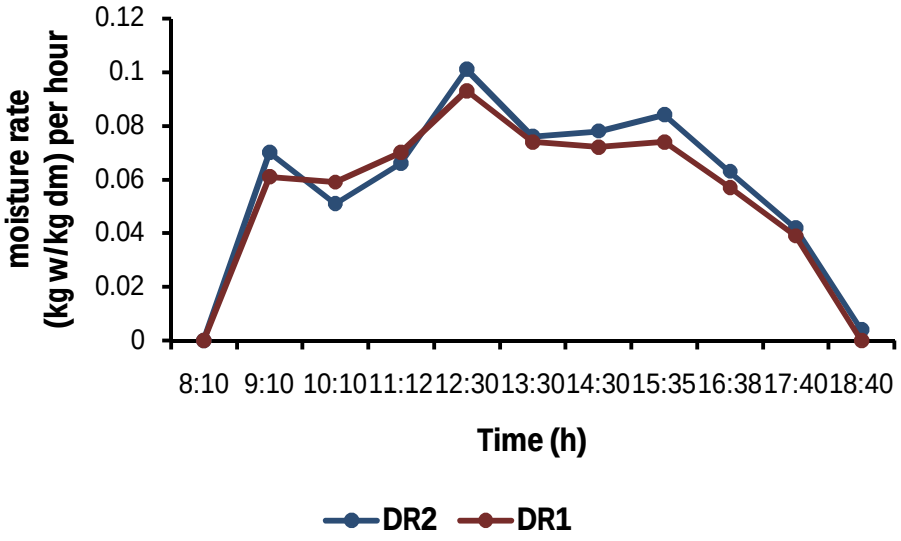

Fig.19. Drying rate variation with the time Test2

4. CONCLUSION

At the end of this work, which involved the design and preliminary study of a solar flour dryer, some important conclusions, lessons and perspectives can be drawn. These include the following

- the solar dryer has been designed, built and studied in a summary manner,
- the drying air in the dryer can heat up to 65°C with natural convection and no load during the unfavourable period chosen for the study,

- with load and forced convection, the average temperature is less than or equal to the lower limit of the predefined drying range,
- the hygrometric and barometric conditions are directly influenced by the thermal conditions and have an impact on the drying process,
- the planned drying time was more than doubled.

Among the lessons to be learnt are the following:

- the approach of designing the solar dryer during unfavourable periods increases the drying time and requires a precise estimation of the solar radiation flux according to the climatic conditions;
- the volume of air under the lowest shelf has a negative effect on drying.

A thorough and complete study of the dryer and the drying process would now be necessary. It would be preferable to eliminate the space under the bottom rack.

REFERENCES

1. Abubakar, S., Umaru, S., Anafi, F. O., & Abubakar, A. S. (2018). Design and Performance Evaluation of a Mixed-Mode Solar Crop Dryer. *FUOYE Journal of Engineering and Technology*, *3*(1), 22–26. https://doi.org/10.46792/fuoyejet.v3i1.133
2. Adelaja, A. O., & Babatope, B. I. (2013). Analysis and Testing of a Natural Convection Solar Dryer for the Tropics. *Journal of Energy*, *2013*, 1–8. https://doi.org/10.1155/2013/479894
3. Ahmed, A., Almas, S., Kissaka, K., & Suleiman, R. (2023). Effect of sun-dry on nutritional and sensory acceptability of wilted African leafy vegetables: a case study of Morogoro Region, Tanzania. *Frontiers in Sustainable Food Systems*, *7*(June), 1–9. https://doi.org/10.3389/fsufs.2023.1161961
4. Ahmed, N., Singh, J., Chauhan, H., Gupta, P., Anjum, A., & Kour, H. (2013). Different drying methods: their applications and recent advances. *International Journal of Food Nutrition and Safety*, *2013*(1), 34–42. https://www.researchgate.net/profile/Dr-Naseer-Ahmed/publication/275650176_Different_Drying_Methods_Their_Applications_and_Recent_Advances/links/554260770cf23ff716835b85/Different-Drying-Methods-Their-Applications-and-Recent-Advances.pdf
5. Alam, M., Saha, C., & Alam, M. (2019). Mechanical drying of paddy using BAU-STR dryer for reducing drying losses in Bangladesh. *Progressive Agriculture*, *30*(1), 42–50. https://doi.org/10.3329/pa.v30i0.41556
6. Babar, O. A., Tarafdar, A., Malakar, S., Arora, V. K., & Nema, P. K. (2020). Design and performance evaluation of a passive flat plate collector solar dryer for agricultural products. *Journal of Food Process Engineering*, *43*(10), 1–13. https://doi.org/10.1111/jfpe.13484
7. Boukaré, O., Boureima, K., Germain, O. W. P., Kalifa, P., & BAHIEBO., D. J. (2024). Practical Exploration of the “Open or Close” Concept: Evaluation of the Hygrothermal Performance of a Bioclimatic Innovation for Onion Bulb Preservation. *Advanced Engineering Forum*, *52*. https://doi.org/accepted journal
8. Burgos, U. De. (2003). BUFFALO. In B. Caballero (Ed.), *Encyclopedia of Food Sciences and Nutrition* (second edi, pp. 2301–2308). Elsevier Science

Ltd. https://doi.org/https://doi.org/10.1016/B0-12-227055-X/00133-4
9. Duffie, J. A., Beckman, W. A., & McGowan, J. (1985). Solar Engineering of Thermal Processes. In *American Journal of Physics* (4th ed., Vol. 53, Issue 4). WILYE. https://doi.org/10.1119/1.14178
10. FORSON, F. K. (1999). *Modelling and experimental investigation of a mixed-mode natural convection solar crop dryer*. Montfort University.
11. Forson, F. K., Nazha, M. A. A., Akuffo, F. O., & Rajakaruna, H. (2007). Design of mixed-mode natural convection solar crop dryers: Application of principles and rules of thumb. *Renewable Energy*, *32*(14), 2306–2319. https://doi.org/10.1016/j.renene.2006.12.003
12. Harrison, J. A., & Andress, E. L. (2000). *Preserving Food: Drying Fruits and Vegetables*. http://nchfp.uga.edu/publications/uga/uga_dry_fruit.pdf
13. Heywood, H. (1971). Operating experiences with solar water heating. *HVE J.*, *29*.
14. Jayas, D. S. (2016). Food Dehydration Basics. In *Food dehydration* (p. 1517). Elsevier. https://doi.org/10.1016/B978-0-08-100596-5.02913-9
15. Khalifa, A. J. N., Al-Dabagh, A. M., & Al-Mehemdi, W. M. (2012). An Experimental Study of Vegetable Solar Drying Systems with and without Auxiliary Heat. *ISRN Renewable Energy*, *2012*, 1–8. https://doi.org/10.5402/2012/789324
16. Khan, M. A., Sabir, M. S., & Iqbal, M. (2011). Development and performance evaluation of forced convection potato solar dryer. *Pakistan Journal of Agricultural Sciences*, *48*(4), 315–320.
17. Krabch, H., Tadili, R., & Idrissi, A. (2022). Design, realization and comparison of three passive solar dryers. Orange drying application for the Rabat site (Morocco). *Results in Engineering*, *15*(July), 100532. https://doi.org/10.1016/j.rineng.2022.100532
18. Lingayat, A., Chandramohan, V. P., & Raju, V. R. K. (2017). Design, Development and Performance of Indirect Type Solar Dryer for Banana Drying. *Energy Procedia*, *109*(November 2016), 409–416. https://doi.org/10.1016/j.egypro.2017.03.041
19. Löf, G. O. G., & Tybout, R. A. (1973). Cost of house heating with solar energy. *Solar Energy*, *14*(3), 253–278. https://doi.org/10.1016/0038-092X(73)90094-7
20. Mishra, S., Verma, S., Chowdhury, S., & Dwivedi, G. (2020). Analysis of recent developments in greenhouse dryer on various parameters- a review. *Materials Today: Proceedings*, *38*(xxxx), 371–377. https://doi.org/10.1016/j.matpr.2020.07.429
21. Moghadam, H., Tabrizi, F. F., & Sharak, A. Z. (2011). Optimization of solar flat collector inclination. *Desalination*, *265*(1–3), 107–111. https://doi.org/10.1016/j.desal.2010.07.039
22. Mohammed, S., Edna, M., & Siraj, K. (2020). The effect of traditional and improved solar drying methods on the sensory quality and nutritional composition of fruits: A case of mangoes and pineapples. *Heliyon*, *6*(6), e04163. https://doi.org/10.1016/j.heliyon.2020.e04163

23. Musembi, M. N., Kiptoo, K. S., & Yuichi, N. (2016). Design and Analysis of Solar Dryer for Mid-Latitude Region. *Energy Procedia*, *100*(September), 98–110. https://doi.org/10.1016/j.egypro.2016.10.145
24. Nizio, E., Czwartkowski, K., & Niedbała, G. (2023). Impact of Smoking Technology on the Quality of Food Products: Absorption of Polycyclic Aromatic Hydrocarbons (PAHs) by Food Products during Smoking. *Sustainability (Switzerland)*, *15*(24), 1–18. https://doi.org/10.3390/su152416890
25. Ojediran, J. O., & Raji, A. O. (2010). Thin layer drying of millet and effect of temperature on drying characteristics. *International Food Research Journal*, *17*(4), 1095–1106.
26. Roy, D., Saha, C. K., Alam, M. A., Sarker, T. R., & Alam, M. M. (2020). Evaluation of s4s solar grain dryer for drying paddy seeds. *Agricultural Engineering International: CIGR Journal*, *22*(4), 200–210.
27. Sehrawat, R., & Nema, P. K. (2018). Low pressure superheated steam drying of onion slices: kinetics and quality comparison with vacuum and hot air drying in an advanced drying unit. *Journal of Food Science and Technology*, *55*(10), 4311–4320. https://doi.org/10.1007/s13197-018-3379-4
28. Stanciu, C., & Stanciu, D. (2014). Optimum tilt angle for flat plate collectors all over the World - A declination dependence formula and comparisons of three solar radiation models. *Energy Conversion and Management*, *81*, 133–143. https://doi.org/10.1016/j.enconman.2014.02.016
29. Yusuf Abdullahi, Y. A. (2013). Performance Evaluation of an Adjustable and Collapsible Natural Convection Solar Food Dryer. *IOSR Journal of Applied Physics*, *3*(3), 8–18. https://doi.org/10.9790/4861-0330818